Synthesis of a New Zirconium Catalyst for Ethylene Polymerization

FABIANA DE C. FIM,[1] TIAGO MACHADO,[2] DENISE SANTOS DE SÁ,[3] PAOLO R. LIVOTTO,[1] ZÊNIS N. DA ROCHA,[3] NARA R. DE S. BASSO,[2] GRISELDA BARRERA GALLAND[1]

[1]Instituto de Química, Universidade Federal do Rio Grande do Sul, Av. Bento Gonçalves 9500, 91501-970 Porto Alegre, Brazil

[2]Faculdade de Química, Pontifícia Universidade Católica do Rio Grande do Sul, Av. Ipiranga 6681, 90619-900 Porto Alegre, Brazil

[3]Instituto de Química, Universidade Federal da Bahia, Campus de Ondina, 40170-290 Salvador, Brazil

Received 14 January 2008; accepted 6 March 2008
DOI: 10.1002/pola.22734
Published online in Wiley InterScience (www.interscience.wiley.com).

ABSTRACT: A novel complex dichlorobis(2-ethyl-3-hydroxy-4-pyrone)zirconium(IV) ($ZrCl_2$(ethylpyrone)$_2$) was synthesized. Complexation of the pyrone ligand to the zirconium was confirmed by UV, ^{1}H and ^{13}C-NMR, and electrochemical studies. NMR showed the presence of four isomers and density functional theory calculations indicated that the main isomer had a cis configuration. The catalyst was shown to be active in ethylene polymerization in the presence of the cocatalyst methylaluminoxane. The highest catalyst activity for the zirconium complex was achieved at Al/Zr = 2500, 70 °C and when a small concentration of catalyst was used (1 μmol). © 2008 Wiley Periodicals, Inc. J Polym Sci Part A: Polym Chem 46: 3830–3841, 2008
Keywords: catalysis; NMR; polyethylene (PE); synthesis; UV-vis spectroscopy

INTRODUCTION

Olefin polymerization catalysis has been increasingly under research interest to develop new catalytic systems capable of competing with Ziegler-Natta and, more recently, with metallocenes. A new generation of postmetallocene catalysts has been proposed in the literature,[1] and some molecules based on bidentate [O,O] ligands have been shown to be active in ethylene polymerization. Flisak and Szczegot[2] studied the strength of co-ordinate bonds in titanium(IV) complexes with three different bidentate ligands of the type [O,O]: tetrahydrofurfurol, tetrahydrofurfuroxo anion, and ethylene glycol dimethyl ether and a complex with the monodentate ligand tetrahydrofuran. The energy required to break one of the bonds of a complex with multidentate ligands with two chemically identical oxygens (such as ethylene glycol dimethyl ether) is almost equal to half of the formation energy. In the complex with the tetrahydrofurfurol ligand (with two different oxygen atoms), the energy required to break the weaker bond is only a small fraction of the total energy of complexation. It may be concluded that the alkoxide anion is a strong donor of electrons that saturate the titanium atom and lower the Lewis acidity of the metal. The easy breakage of one of the alkoxide bonds leads to the formation of complexes with monodentate dangling ligands, which seem vital in the process of polymerization. Moreover, these complexes present the highest catalytic activity in the ethylene poly-

Correspondence to: (E-mail: griselda@iq.ufrgs.br)
Journal of Polymer Science: Part A: Polymer Chemistry, Vol. 46, 3830–3841 (2008)

merization, with a higher activity than those of the catalysts with bidentate ligands with equal donor power.

In 1995, Schaverien and coworkers[3] published a study with several titanium and zirconium complexes with sterically hindered chelating phenoxide ligands as catalysts for the olefin polymerization. Recently, Eisen and coworkers[4] synthesized a dimeric titanium complex with ethoxide group bridges; this complex was tested for ethylene and propylene polymerizations in the presence of methylaluminoxane (MAO). The propylene obtained presented an intermediate tacticity and high molecular weight. Eisen and coworkers[5] also synthesized various complexes of group 4 metals with the ligand acetyl acetonate with different substituents and tested for the polymerization of propylene in the presence of MAO. All the complexes were active and produced elastomeric polypropylene.

Other bidentate alkoxide ligands are the derivates of maltol, also known as 3-hydroxy-2-methyl-4-pyrone (maltol) and 2-ethyl-3-hydroxy-4-pyrone (ethylmaltol). When maltol is desprotonated (pKa = 8.38), an anionic system is formed, which is capable of acting as a chelating, bidentate ligand of the type [O,O]. As such, this ligand has two different oxygen donors and can be considered as an anionic AB bidentate ligand.[6] Titanium complexes based in maltolato and guaicolato ligands with an octahedral coordination were synthesized by Sobota et al.[7] and tested for ethylene polymerization. In all complexes the titanium atoms were surrounded by four oxygen atoms from the chelating maltolato or guaicolato ligands and by two mutual cis chlorine or ethoxide groups. Electrochemical studies showed that the maltolato ligand behaves as a weaker electron donor than the guaicolato ligand and forms mononuclear complexes of Ti(IV) that are less stable in electrolytic solutions (dimerization occurs with maltol liberation) but more stable in the Ti(III) complexes derived on reduction. With regard to ethoxide and chloride ligands electrochemical studies show that these complexes exhibit identical electron-donor abilities as indicated by their identical reduction potentials or by their reversible cathodic waves in the mononuclear complexes; however, the substitution of chlorine with ethoxide ligands decreases the catalytic activity of these complexes. In a previous study[8] we obtained bidentate zirconium complexes of maltol and naphtoquinone that presented a coordination of the two oxygen atoms with the metal to produce a chelating ring of five members. Both complexes were shown to be active in the ethylene polymerization producing high-molecular-weight polyethylene. In another study[9] the titanium complex of maltol was grafted on to different inorganic supports attaining higher catalytic activities than those obtained with the homogeneous complex. In the present work, we synthesized the complex, dichlorobis(2-ethyl-3-hydroxy-4-pyrone)zirconium(IV) ($ZrCl_2$(ethylpyrone)$_2$) and investigated its reactivity and stability by cyclic and pulse voltammetry. In addition, the catalytic activity in this complex was determined during ethylene polymerization in the presence of MAO and compared with the catalyst dichlorobis(3-hydroxy-2-methyl-4-pyrone)zirconnium(IV) ($ZrCl_2$(methylpyrone)$_2$).

EXPERIMENTAL

General Procedures

All experiments were performed under argon atmosphere using the Schlenk technique. All the solvents were dried by usual methods existing in the literature. Acetonitrile was refluxed for 6 h followed by distillation and kept under molecular sieve. Tetrabutylammonium tetrafluoroborate (Merck or Fluka) was purified through successive extractions with ethyl acetate at 78 °C. The crystals were collected by filtration and vacuum-dried. MAO (Witco, 12.9% w/w Al in toluene solution) was employed as received. The ligand 2-ethyl-3-hydroxy-4-pyrone (Aldrich) and $ZrCl_4$ (Merck) were used without further purification.

Synthesis of Dichlorobis(2-ethyl-3-hydroxy-4-pyrone)zirconium(IV)

The complex was synthesized by three methods that differ in the preparation of the $ZrCl_4$ suspension in tetrahydrofuran (THF). Method 1: THF was added drop wise to $ZrCl_4$. Method 2: Little portions of $ZrCl_4$ were added to THF. Method 3: An adduct of $ZrCl_4$ and THF was prepared in the following way: 10 mL of THF were added drop wise at room temperature, to a stirred suspension of 8.8 g (37.8 mmol) of $ZrCl_4$ in 100 mL of dichloromethane in a Schlenk sob inert atmosphere. After 2 h, the white solution was transferred with a syringe to other Schlenk with a fritted disk. 80 mL of hexane were added

to the filtered solution and the white solid obtained was washed three times with 15 mL of hexane and dried under vacuum.

Preparation of the Complex

The ligand 2-ethyl-3-hydroxy-4-pyrone (1.00 g, 7.14 mmol) in solution of THF was added drop wise to a stirred suspension of $ZrCl_4$ (0.83 g, 3.56 mmol) in THF (methods 1 and 2) or to the adduct (method 3). The mixture was stirred at room temperature for 60 min, then filtered, and washed with diethyl ether (3 × 5 mL). The product was dissolved in CH_2Cl_2 (10 mL) and hexane (40 mL) was added to give a yellow precipitate, which was filtered, washed with hexane (3 × 5 mL), and dried under vacuum. The yield of the complex was 82% (method 1), 91% (method 2), and 92% (method 3). Anal. Found: C, 38.19; H, 3.18. Calcd. for $C_{14}H_{14}O_6Cl_2Zr$: C, 37.27; H, 3.75. ^{1}H-NMR (300 MHz, DMSO-d_6): δ = 8.56 ppm (d, 2Ha, J_{HH} = 5 Hz, Ha - isomer A), δ = 8.51 ppm (d, 2Ha, J_{HH} = 5 Hz, Ha - isomer B), δ = 8.42 ppm (d, 2Ha, J_{HH} = 5 Hz, Ha - isomer C), δ = 8.36 ppm (d, 2Ha, J_{HH} = 5 Hz, Ha - isomer D), δ = 6.81 ppm (d, 2Hb, J_{HH} = 5.1 Hz, Hb - isomer B), δ = 6.76 ppm (d, 2Hb, J_{HH} = 5.1 Hz, Hb - isomer A), δ = 6.72 ppm (d, 2Hb, J_{HH} = 5.1 Hz, Hb - isomer D), δ = 6.63 ppm (d, 2Hb, J_{HH} = 5.1 Hz, Hb - isomer C); δ = 2.68 ppm (q, 4H, J_{HH} = 6Hz, CH_2), δ = 2.61 ppm (q, 4H, J_{HH} = 6 Hz, CH_2); δ = 1.08 ppm (t, 6H, J_{HH} = 6Hz, CH_3), δ = 1.04 ppm (t, 6H, J_{HH} = 6Hz, CH_3). ^{13}C-NMR (300 MHz, DMSO-d_6): δ = 180.97 ppm (C_c—C=O, isomer C), δ = 180.19 ppm (C_c—C=O, isomer B), δ = 179.91 ppm (C_c—C=O, isomer D); δ = 158.06 ppm (C_a), δ = 157.08 ppm (C_a); δ = 156.10 ppm (C_d), δ = 155.22 ppm (C_d); δ = 153.65 ppm (C_e), δ = 153.26 ppm (C_e); δ = 110.16 ppm (C_b), δ = 109.88 ppm (C_b); δ = 21.77 ppm (CH_2), δ = 21.63 ppm (CH_2), δ = 21.49 ppm (CH_2); δ = 11.66 ppm (CH_3).

Complex Characterization

The NMR spectra of the complex were recorded on a Varian Inova 300 spectrometer, using DMSO-d_6 as solvent. The UV spectra of the ligand and the complex were recorded on a UV-Vis spectrophotometer UV-1601PC Shimadzu, using a special cell with inert atmosphere. The analysis were performed using a concentration of 5.5 × 10^{-4} M in toluene as solvent. Elemental analysis (C, H) was made with a Fisons EA 1108 microanalyzer.

Cyclic Voltammetry

The cyclic voltammetry (CV), differential pulse voltammetry (DPV) and controlled potential electrolysis (CPE) (coulometry) measurements were taken with a potentiostat/galvanostat (PARC, model 273). All experiments were carried out using a conventional three electrodes cell. Glassy carbon was used as working electrode for CV and platinium gauze for coulometry. An Ag/AgCl electrode was used as the reference electrode and a platinum wire as the auxiliary electrode. Ag/AgCl electrode was calibrated by ferrocene, used as an internal reference. These measurements versus the ferrocene (Fc^+/Fc^0) redox couple (+0.50 V in acetonitrile solutions) and were reported versus an Ag/AgCl electrode. Electrochemical data were obtained using 0.1 mol L^{-1} solutions of tetrabutylammonium tetrafluoroborate in acetonitrile as supporting electrolyte. In the cyclic voltammograms or differential pulse, neither anodic nor cathodic peaks were observed in the absence of titanium or zirconium complexes in the potential range studied. All solutions were deaerated by bubbling high purity argon. The cocatalyst solutions were prepared with different Al/Zr molar ratios between 0 and 10 and the cyclic voltammograms were recorded with scan rate of 100 mV s^{-1}. The electronic absorption spectra were recorded using Hewlett-Packard Modeles 8453. Successive spectra were recorded during the redox process of the complexes.

Theoretical Calculations

The energy of all calculated species was obtained by full geometry optimization without any constrain. The calculations were performed with the Gaussian 98 Program,[10] at a HF/B3LYP[11,12] level of theory, using a Dunning-Huzinaga DZ95[13] basis set complemented with polarization functions for the nonmetal atoms and a DZ valence basis set plus an effective core potential[14–16] for the zirconium.

Polymerization Reactions

Ethylene polymerizations were performed using a 0.3L of toluene in a 1.0L Pyrex glass reactor connected to a constant temperature circulator, with an internal temperature indicator,

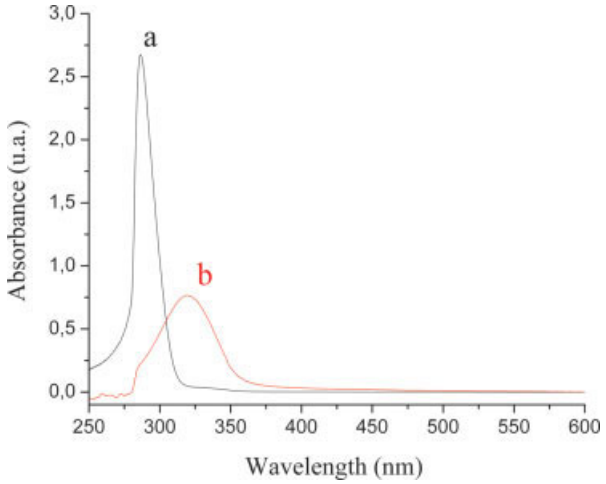

Figure 1. UV-vis spectra in toluene at ambient temperature using a concentration of ligand and of the zirconium complex of 5.5×10^{-4} M. [Color figure can be viewed in the online issue, which is available at www.interscience.wiley.com.]

equipped with mechanical stirring and inlets for argon and the monomer. MAO was used as cocatalyst in a Al/Zr molar ratio of 1000, 2500, 3500, and 4500. For each experiment, a mass of catalyst system corresponding to 1 or 10 μmol of Zr was suspended in toluene and transferred into the reactor under argon. The polymerization reactions were carried out under 1.6 bar of ethylene pressure, at 30, 40, 60, 70, or 80 °C during 60 min. The reagents were introduced in the reactor in the following order: solvent, cocatalyst, ethylene, and catalyst solution. Acidified (HCl) ethanol was used to quench the process, and reaction products were separated by filtration, washed with distilled water, and dried under reduced pressure at room temperature.

Polymer Characterization

The melting points (T_m) of the polymers were determined using a differential scanning calorimeter (Perkin–Elmer, DSC-4), at a heating and cooling rate of 10°C min^{-1} in the temperature range of 30-160 °C. The heating cycle was performed twice, but only the results of the last scan were considered. Molar masses and molar mass distributions were measured by high temperature gel permeation (GPC) using a 150C Waters instrument, equipped with a differential refractometer and HT Styragel columns (HT3, HT4 and HT6). 1,2,4-Trichlorobenzene was used as mobile phase at a flow rate of 1 mL min^{-1}. The analysis was performed at 135 °C.

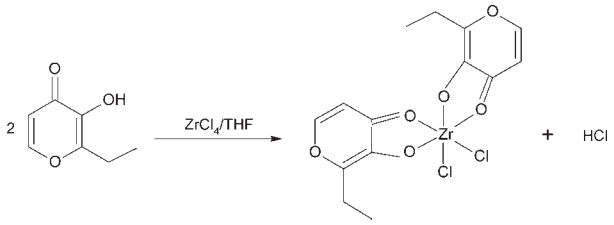

Scheme 1. Synthesis of dichlorobis(2-ethyl-3-hydroxy-4-pyrone)zirconium(IV).

RESULTS AND DISCUSSION

The ligand 2-ethyl-3-hydroxy-4-pyrone is an α,β-unsaturated enone, whose $\pi \rightarrow \pi^*$ electronic transition absorbs at 286 nm ($\varepsilon_{max} = 4900$ mol^{-1} L cm^{-1}), as can be seen in Figure 1(a). The UV spectrum of the zirconium complex shows [Fig. 1(b)] the disappearance of this band, due to the loss of conjugation of the enone, demonstrating the complexation of the metal by the carbonyl group. In contrast, another absorption peak appears in the UV spectrum at 320 nm ($\varepsilon_{max} =$ 1360 mol^{-1} L cm^{-1}), which may be attributed to a ligand-to-metal charge transfer from π type orbital of the pyrone ligand to the d^0 orbital of the zirconium.[17] The low intensity of this band can be attributed to a low superposition between the metal and ligand orbitals.[18,19] The complex obtained is demonstrated in Scheme 1.

Figure 2(a,b) shows the ^{1}H-NMR spectra of the ligand and the complex respectively. The resonance of the hydroxyl group ligand disappears at 8.83 ppm in the complex spectrum showing the desprotonation of the ligand due to the metal insertion. The shift of Ha and Hb protons in the complex to higher frequencies in relation to the resonance ligand demonstrates

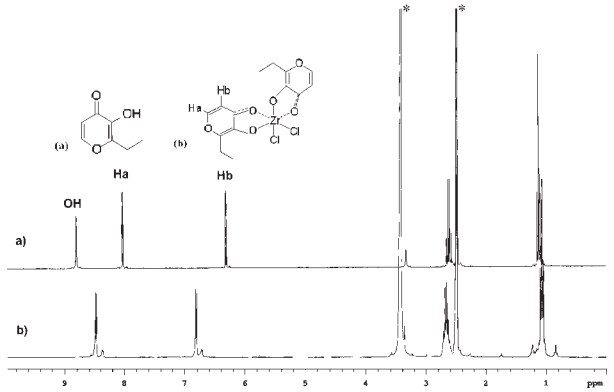

Figure 2. ^{1}H-NMR spectra of (a) the ligand 2-ethyl-3-hydroxy-4-pyrone and (b) the zirconium complex. *DMSO.

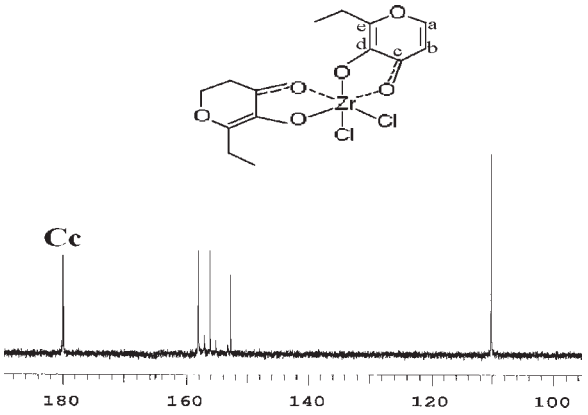

Figure 3. ^{13}C-NMR spectrum of the zirconium complex (the aliphatic region is not shown).

the desblindage of the aromatic protons due to the donation of electronic density to the metal.

The ^{13}C-NMR of the complex (Fig. 3) shows the carbonyl signal (Cc) at 180 ppm and a series of signals in the aromatic region. To assign all the carbon atoms Heteronuclear Correlation Spectroscopy (HETCOR) was performed and the spectrum is shown in Figure 4. This technique permits the identification of unmistakable protons **a** and **b**. Carbons **d** and **e** do not show signals in HETCOR since they are quaternary carbons, carbon **d** appears at higher frequencies than carbon **e** because of the influence of the carbonyl directly bonded to it.

The ^{1}H-NMR, as well as the ^{13}C-NMR, spectra show the presence of isomers. The ^{1}H-NMR shows the presence of four isomers that vary in proportion depending on the method of synthesis. In fact, Figure 5 shows the expanded spectra of the Ha and Hb proton region for the complexes obtained with the different methods of synthesis. The resonance of proton Ha in the ^{1}H-NMR was quantified to study the proportion of the isomers and their stability. In a previous study, the dichlorobis(3-hydroxy-2-methyl-4-pyrone)zirconium(IV) complex showed an interconvertion between isomers in DMSO.[20] Studies on the stability of the dichlorobis (2-ethyl-3-hydroxy-4-pyrone)zirconium(IV) isomers in DMSO showed that the isomers are stable after more than 16 h in solution. The proportion of these different isomers was calculated from the integral of protons **a,** as shown in Table 1. The first synthesis produced two main isomers almost in the same proportion, while the other two syntheses resulted in one main isomer, indicating that by changing the synthetic path it is possible to modify the isomer proportion. As such, isomer proportion appears to be related to the kinetics of the synthesis. In fact, in the first two methods, the ligand is reacted with a suspension of $ZrCl_4$ in THF that probably has a kinetic control and in the third synthesis the ligand is reacted with the adduct that is soluble in THF, with this reaction being controlled thermodynamically to give the most stable isomer.

The complex was formed as a powder and despite a number of attempts, it was not possible to obtain a single crystal to achieve an X ray diffractogram to elucidate the complex's structure. As such, a theoretical study was performed on the complex by the density functional theory (DFT) method, which demonstrated 10 possible isomer/conformers, 6 with the cis configuration and 4 with the trans configuration with respect to the position of the chlorine atoms. These different possibilities are shown in Figure 6. The *cis* 11, 12, and 13 structures are conformers, as are structures *cis* 21, 22, and 23. The trans isomers also have conformers *trans* 11 and 12 and *trans* 21 and 22. Table 2 presents the relative energies of the isomer/conformers and the relative population considering a temperature of 298 K and a distribution in the vacuum. Given the proportion of isomers given by NMR with the energies depicted in Table 2 and taking into consideration that the conformers are not distinguishable by NMR at room temperature, it may be speculated that the main isomer is *cis*1 (isomer B), the second most abundant isomer is *cis*2 (isomer D), and the less abundant isomers are *trans*1 (isomer C) and *trans*2 (isomer A).

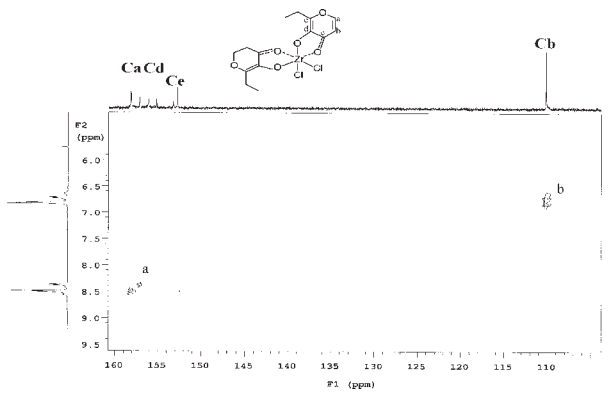

Figure 4. HETCOR spectrum of the zirconium complex (the aliphatic region is not shown).

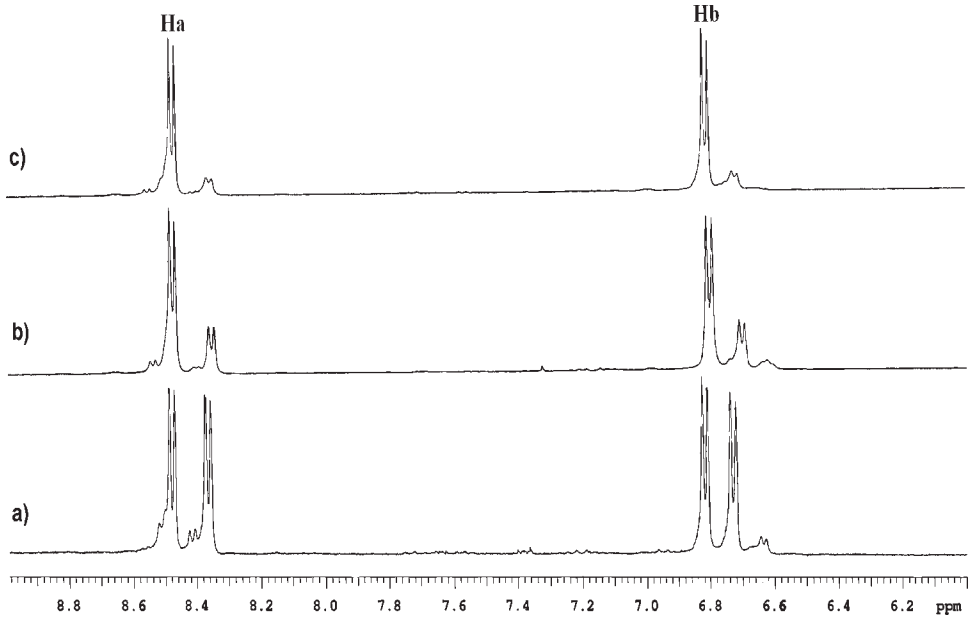

Figure 5. ^{1}H-NMR spectra (expanded region) of the zirconium complex obtained by (a) method 1, (b) method 2, and (c) method 3.

Electrochemical Behavior

The electrochemical behavior of dichlorobis(2-ethyl-3-hydroxy-4-pyrone)zirconium(IV) was investigated through CV and DPV and CPE. The cyclic and pulse voltammograms were run over a potential range of between 0.2 V and −2.6 V with a scan rate of 100 mV s^{-1}. Figure 7(a,b) shows the pulse voltammograms with cathodic and anodic scans for the complex $ZrCl_2$(ethylpyrone)$_2$ and the pyrone ligand, which demonstrated the reversibility of each reduction process. The curves show the pyrone ligand cathodic and anodic processes at −2.0 e −2.6 V versus Ag/AgCl, and the complex at −1.3 (asymmetric signal) and at −1.95, −2.6 and a shoulder at −1.6. Comparing the curves of current versus potential of the ligand and the complex it can be seen that the signals at −1.95 and −2.6 V in the complex voltammogram correspond to the redox processes of the ligand, L/L^- and L^-/L^{2-}. The other signals are due to the redox processes of the metal center. These results are similar to those obtained with the $ZrCl_2$(methylpyrone)$_2$ analog complex,[20] which demonstrated cathodic waves at −1.3, −1.8, and −2.1 V. Comparing the results obtained with both $ZrCl_2$(pyrone)$_2$ (methyl or ethyl) complexes, it may be concluded that the nature of the alkyl group has no influence on the electronic density of Zr(IV), since the reduction potentials of the metallic center are similar in both complexes (Fig. 8). It is worth noticing that, in the −1.3 V region of the complex $ZrCl_2$(ethylpyrone)$_2$ there is a nonsymmetric signal, with the appearance of two cathodic waves at −1.25 V and −1.35 V. This asymmetry may be due to the presence of a higher number of isomers or conformers for the $ZrCl_2$(ethylpyrone)$_2$ complex than for the $ZrCl_2$(methylpyrone)$_2$ complex, which is in accordance with the NMR results.[20]

Table 1. Proportion of Different Isomers of Complex Dichlorobis(2-ethyl-3-hydroxy-4-pyrone)zirconium(IV) Obtained by the Integral of the ^{1}H NMR Spectrum of Proton **a**

	% Isomer A (8.56 ppm)	% Isomer B (8.51 ppm)	% Isomer C (8.42 ppm)	% Isomer D (8.36 ppm)
Method 1	≅0	47.7	6.8	45.5
Method 2	7.1	67.5	3.6	21.8
Method 3	5.4	81.6	0	13.0

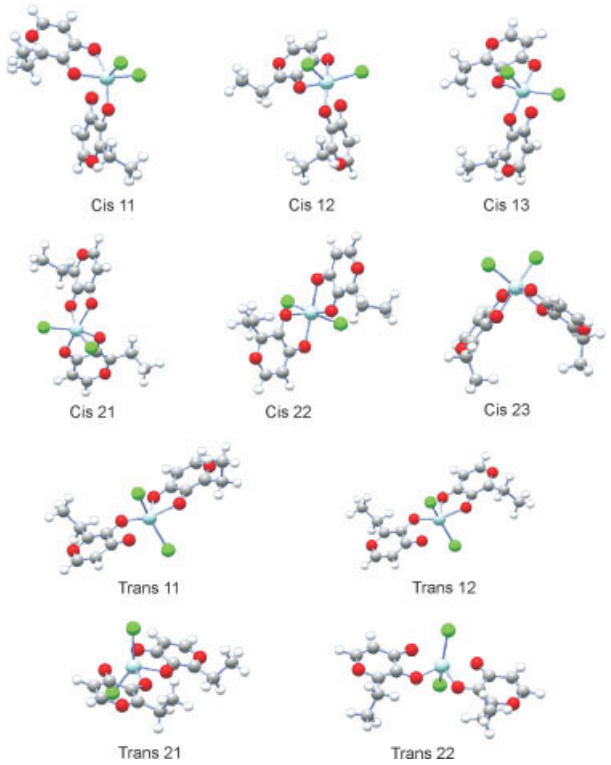

Figure 6. Structures of the 10 possible isomers/conformers of complex dichlorobis(2-ethyl-3-hydroxy-4-pyrone)zirconium(IV).

The results obtained for the $ZrCl_2$(ethylpyrone)$_2$ complex at controlled potential (−1.7 V) with the consumption of 2 F mol^{-1} suggest that charge-transfer process involves two electrons. These results were important for attributing the cathodic and anodic signals centered in the ligand and in the zirconium and the electrode mechanism. Thus, considering the bi-electronic process the waves at −1.3 V and −1.6 V can be assigned to $Zr^{IV/III}$ and $Zr^{III/II}$ reduction processes.

The CPE results indicate that the electrode processes of the $ZrCl_2$(ethylpyrone)$_2$ complex are reversible with a chemical coupled reaction. Data suggest that, after the reduction of Zr(IV), there is a labilization of the ethylpyrone ligand.

The differential pulse voltammogram for $ZrCl_2$(ethylpyrone)$_2$ recorded after electrolysis shows the disappearance of the redox processes centered at the metal as shown in Figure 9, as a consequence of the chemical reaction concomitant with the reduction of Zr(IV) in the original complex. In this curve, the existence of cathodic signals (−2.1 e −2.5 V) corresponding to the reduction of the noncoordinated ligand can be seen [Fig. 9(b)]. The signal around at −0.7 V [Fig. 9(b)] probably results from a Zr(II) complex coordinated to a Lewis base, acetonitrile or pyrone. For a more accurate explanation of the electrolysis product, further studies will be necessary.

All the previous data for the $ZrCl_2$(ethylpyrone)$_2$ complex permits the proposal of the equations listed in Scheme 2 for the electrode mechanism. Equations 1, 2, and 4 are related to the redox processes at the metallic center and eq 3 refers to the redox process of the ligand.

To investigate the electrochemical behavior of $ZrCl_2$(ethylpyrone)$_2$ in the presence of MAO, we carried out differential pulse and cyclic voltametric measurements under an ethylene atmosphere, using an Al/Zr molar ratio of 5. The differential pulse (Fig. 10) and cyclic voltammogram (Fig. 11) profiles of the complex $ZrCl_2$(ethylpyrone)$_2$, in the presence of MAO, show the disappearance of the anodic and cathodic waves centered at the zirconium; however, there are no other signals that could be attributed, definitely, to the substitution of Cl^- by $—CH_3$. In the presence of ethylene a signal appears at around −0.8 V, which can be attributed to the methylated active species. This result indicates that the active specie seems to be stabilized by the ethylene atmosphere. The successive cyclic voltammograms recorded with scan rate 200 mV s^{-1} (Fig. 11) show that the current peak at −0.8 V for Al/Zr = 5 decreases with time, probably due to the inability of these active species in solution. The best results for the CV in the presence of MAO, were observed when the Al/Zr ratio was 5, since below this ra-

Table 2. Relative Energies and Populations of the 10 Possible Isomers/Conformers of the Complex Dichlorobis(2-ethyl-3-hydroxy-4-pyrone)zirconium(IV)

Isomer/Conformer	Relative Energy (kcal/mol)	Population (%)
Cis11	0.000	27.62
Cis12	0.072	48.94
Cis13	0.150	21.43
Cis21	2.324	0.55
Cis22	2.454	0.88
Cis23	2.659	0.30
Trans11	5.669	<0.01
Trans12	5.652	<0.01
Trans21	3.552	0.11
Trans22	3.501	0.14

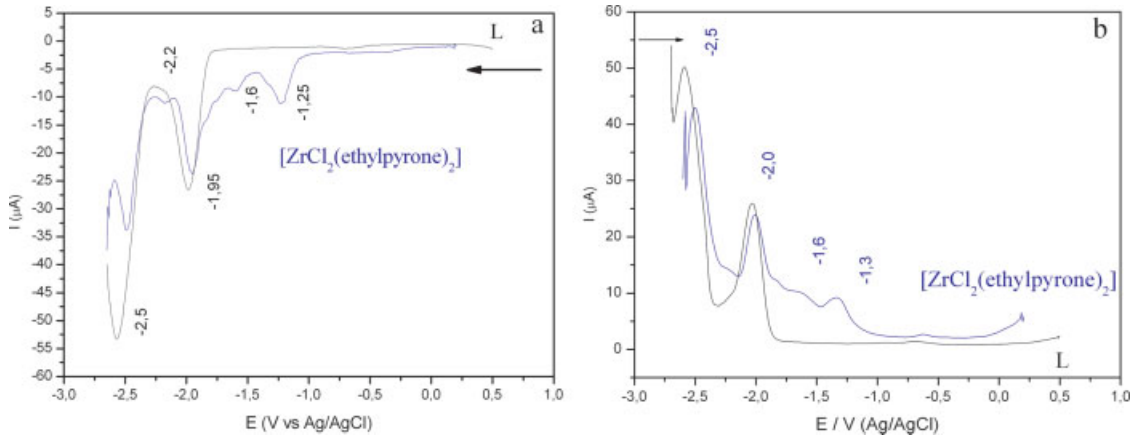

Figure 7. Pulse voltammograms of complex $ZrCl_2$(ethylpyrone)$_2$: (a) cathodic scan of the complex and the ligand; (b) anodic scan; v = 100 mV s^{-1}. [Color figure can be viewed in the online issue, which is available at www.interscience.wiley.com.]

tio the signal at −0.8 V could not be appreciated and at higher ratios the modification of the signal was too fast. The increase in the Al/Zr ratio did not present a modification of the redox potential of $Zr^{IV/III}$ in the active specie at −0.8 V, thus it can be deduced that in the coordination sphere of Zr(IV), methyl and ethylene are present.

Ethylene Polymerization

The effect of the polymerization temperature on the catalytic activity of the dichlorobis(2-ethyl-3-hydroxy-4-pyrone)zirconium(IV) complex was evaluated and the results are shown in Figure 12. The catalytic activity increased when the temperature was increased from 30 to 60 °C for both Al/Zr ratios used. The catalytic activity decreased above 60 °C when 10 μmol of Zr and a ratio of Al/Zr of 1000 were used but when a higher amount of MAO was used, the catalytic activity only decreased above 70 °C. The presence of higher amounts of MAO helps to stabilize the active species at higher temperatures. In general, postmetalocene catalysts are easily deactivated by temperature;[21] however, the dichlorobis(2-ethyl-3-hydroxy-4-pyrone)zirconium(IV) complex showed the best performance at 70 °C, demonstrating a high stability of this complex.

The effect of the Al/Zr ratio on the catalytic activity of the 1 μmol of zirconium complex during ethylene polymerization was also studied at 60 °C. The results are shown in Figure 13. The complex showed the best catalytic activity when the Al/Zr ratio was 2500. The increase from 2500 to 4500 decreased the catalytic activity,

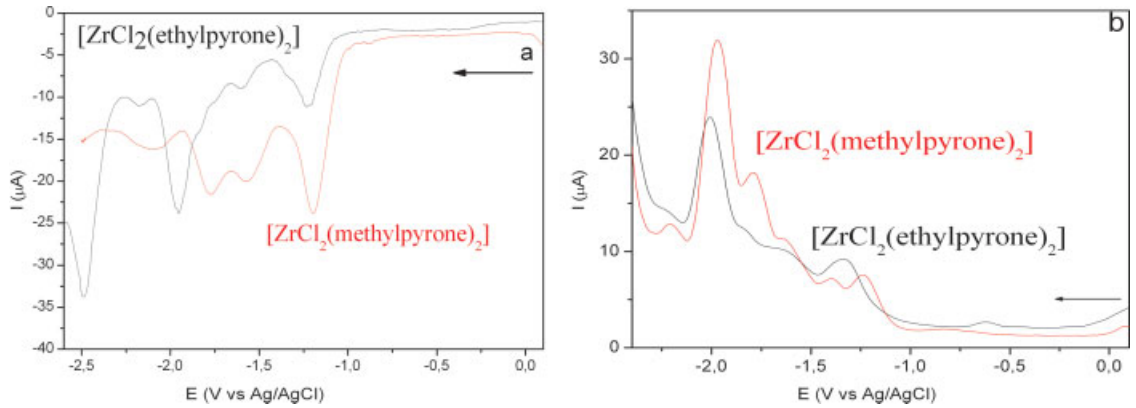

Figure 8. Pulse voltammogram of complexes $ZrCl_2$(methylpyrone)$_2$ and $ZrCl_2$(ethylpyrone)$_2$: (a) cathodic scan of the complex and the ligand; (b) anodic scan; v = 100 mV s^{-1}. [Color figure can be viewed in the online issue, which is available at www.interscience.wiley.com.]

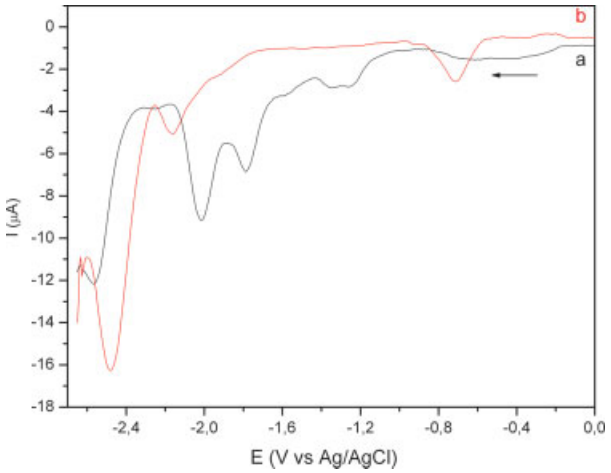

Figure 9. Cyclic voltammograms of the complex $ZrCl_2$(ethylpyrone)$_2$: (a) initial; (b) electrolyzed ($E_{applied} = -1.7$ V). [Color figure can be viewed in the online issue, which is available at www.interscience.wiley.com.]

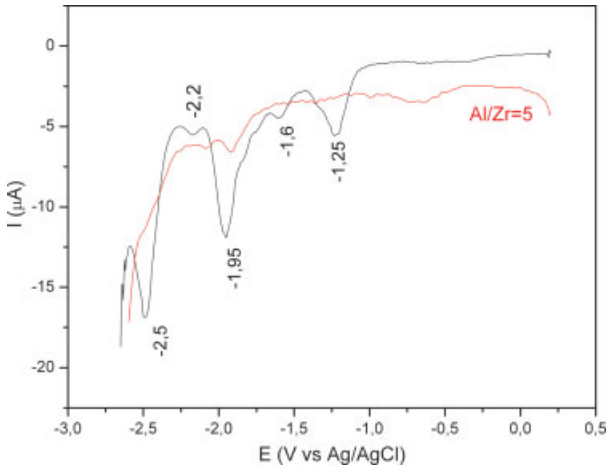

Figure 10. Pulse voltammogram of complex $ZrCl_2$(ethylpyrone)$_2$ in the presence of MAO (Al/Ti = 5) and in ethylene atmosphere. [Color figure can be viewed in the online issue, which is available at www.interscience.wiley.com.]

suggesting that high amounts of MAO can compete with the olefin for the active site of the complex, decreasing the activity.[22]

The complexes obtained by the three synthetic methods were compared in the ethylene polymerization under the same reaction conditions. The results of catalytic activity are shown in Figure 14. Method 3, in which the complex is obtained from the zirconium adduct, presented the best result, probably due to the fact that the complex is formed mainly by the cis isomers and contain the lowest number of trans isomers, which are not expected to be active in olefin polymerization. This catalytic activity result confirms that the isomer determination performed by NMR and DFT is correct.

The ^{13}C-NMR analysis of the polyethylene obtained in the polymerization reactions showed a single resonance at 30 ppm, indicating that the polymers are linear and that no branching is observed. The set of evaluated polymerization conditions, as well as polymer melting temperatures and molecular weights, are presented in Table 3. The results were obtained with the complex synthesized by method 2. The best activity obtained was 310 kgPE/molZr.h.atm when Al/Zr = 2500 was used and a temperature of 70 °C (entry 9).

The complex was shown to be more active when a smaller amount of catalyst was used, as can be seen for entries 3 and 11 or 5 and 8. A similar finding has also been reported in the literature for other catalytic systems.[23]

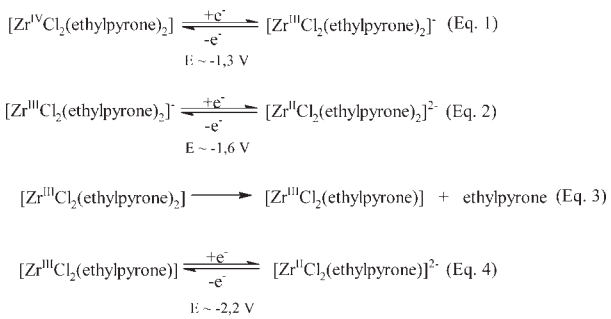

Scheme 2. Redox process of the complex $ZrCl_2$(ethylpyrone)$_2$.

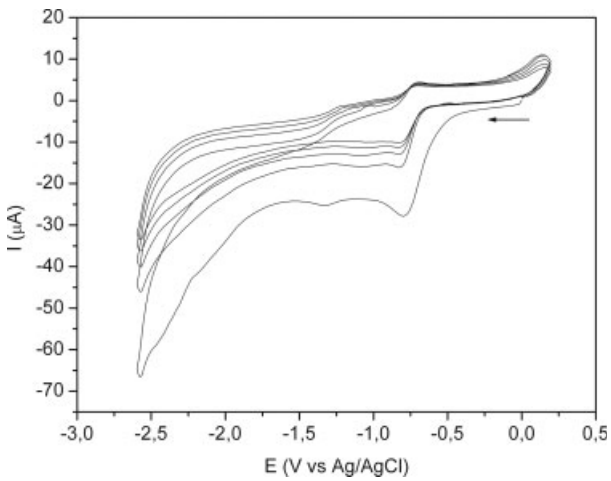

Figure 11. Successive cyclic voltammograms of complex $ZrCl_2$(ethylpyrone)$_2$ at Al/Zr = 5 in ethylene atmosphere. $v = 200$ mV s^{-1} and $T = 25$ °C.

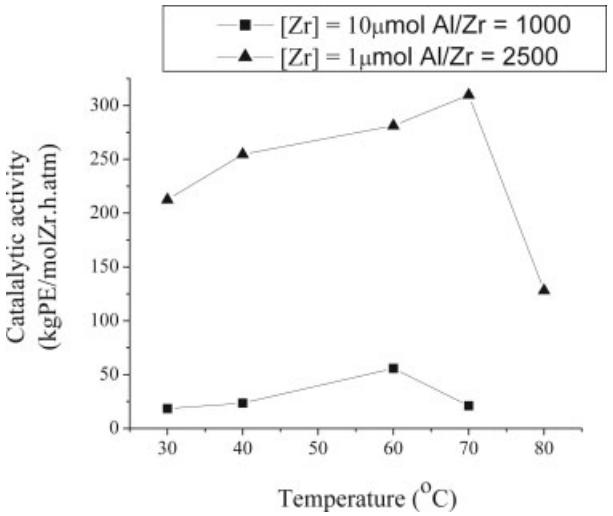

Figure 12. Influence of the polymerization temperature in the catalytic activity of the complex dichlorobis (2-ethyl-3-hydroxy-4-pyrone)zirconium(IV) (method 2).

The DSC results showed that the polymers obtained have melting points of between 130 and 134 °C, typical of high density polyethylene. GPC results showed high-molecular-weight polyethylene with a narrow distribution of molecular weight. However, the products had to be filtered to perform the GPC analyses and some of them did not solubilize at all. In fact, the molecular weight (Mw) of the soluble part was very high, suggesting that the polyethylene could have a fraction with an ultra high molecular weight. The dicholorobis(3-hydroxy-2-methyl-4-pyrone)-zirconium(IV) complex produced polymers that were so insoluble that it was not possible to obtain the molecular weight by GPC.

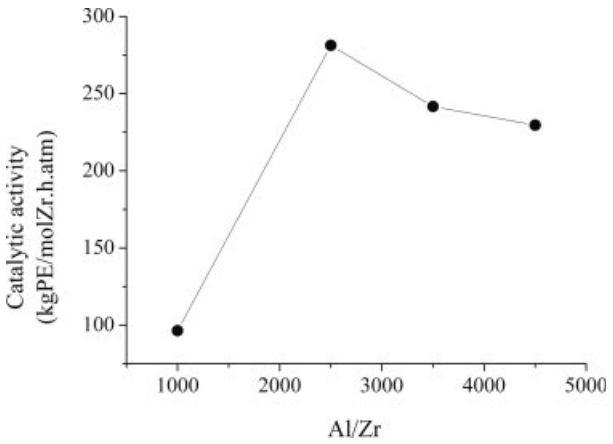

Figure 13. Influence of the Al/Zr ratio in the catalytic activity of the complex dichlorobis(2-ethyl-3-hydroxy-4-pyrone)zirconium(IV) (method 2).

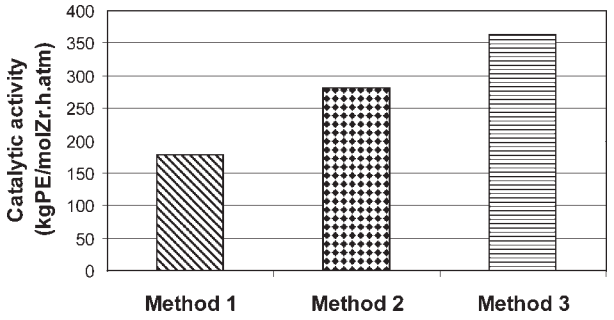

Figure 14. Comparison of the catalytic activities in the ethylene polymerization with the ethyl pyrone zirconium complex obtained by the three synthetic methods. ([Zr] = 1 μmol, Al/Zr = 2500, T = 60 °C, P_{etileno} = 1.6 atm, solvent = toluene, and t = 60 min)

The comparison between the catalytic activities of the $ZrCl_2$(ethylpyrone)$_2$] **(I)** and [$ZrCl_2$(methylpyrone)$_2$] **(II)**) complexes (Fig. 15) showed that the complex **(I)** is much more active. The increase in catalytic activity can be attributed to the presence of the ethyl group in the 2-ethyl-3-hydroxy-4-pyrone ligand. Since the electrolysis studies, showed that there is no electronic effect when the methyl group is changed by the ethyl group in this kind of complex, the difference can be attributed to a steric effect. Morokuma and coworkers[24] studied the effect of substituents in zirconium catalysts with alkoxy bidentate ligands and concluded that the steric effect, due to bulky substituents, significantly change the geometry of the π-complexes (present in the polymerization mechanism) and produce changes in the electronic energies. The steric interaction produces a greater change in the energy of the π-complex than in the transition state, resulting in a decrease in the energy of the ethylene insertion, increasing the catalytic activity of the system. Another hypothesis that may justify the increase in activity from complex II to I is that since the $ZrCl_2$(ethylpyrone)$_2$ is more soluble in toluene than $ZrCl_2$(methylpyrone)$_2$ this will favor the diffusion of the species to the active center.

CONCLUSIONS

A new zirconium complex dichlorobis(2-ethyl-3-hydroxy-4-pyrone)zirconium(IV) with bidentate alkoxide ligands was synthesized and characterized by ^{1}H and ^{13}C-NMR, HETCOR, UV, and electrochemistry. UV showed the complexation of the ligand. NMR studies showed the presence

Table 3. Catalytic Activity and Properties of the Ethylene Polymerization Catalyzed by Dichlorobis (2-ethyl-3-hydroxy-4-pyrone)zirconium(IV)

Entry	[Zr] (μmol)	Al/Zr	T (°C)	Polymer (g)	Activity[a]	T_m (°C)	M_w (10^3 g mol^{-1})	M_w/M_n
1	10	1000	30	0.29	18	131	400	1.9
2	10	1000	40	0.38	24	134	i	i
3	10	1000	60	0.89	56	130	150	4.2
4	10	1000	70	0.34	21	134	nd	nd
5	10	2500	60	2.98	186	133	503	1.4
6	1	2500	30	0.34	213	132	i	i
7	1	2500	40	0.41	255	132	428	2.0
8	1	2500	60	0.45	281	132	317	2.6
9	1	2500	70	0.50	310	132	nd	nd
10	1	2500	80	0.20	128	134	nd	nd
11	1	1000	60	0.16	96	132	i	i
12	1	3500	60	0.39	242	133	nd	nd
13	1	4500	60	0.37	230	134	nd	nd

i, insoluble; nd, not determined; $P_{Ethylene}$ = 1.6 atm; solvent = toluene; time = 1 h.
[a] kgPE/molZr.h.atm.

of four isomers, with the cis configuration being the most abundant and stable. The results of the electrochemical studies showed that the nature of the alkyl group (methyl or ethyl) in the pyrone ring did not influence the electronic density of Zr(IV) and that the active species are stabilized by an ethylene atmosphere. The complex was active for ethylene polymerization, cocatalyzed by MAO, giving the best catalytic activities at 70 °C, Al/Zr = 2500 and [catalyst] = 1 mmol. Complex I showed a better performance in ethylene polymerization that the complex with a methyl group.

Taking into account the electrochemical studies of the complex, it is reasonable to conclude that the high catalytic activity of $ZrCl_2$(ethylpyrone)$_2$ is related to the fact that Zr(IV) is stable. Furthermore, cyclic and differential pulses illustrated the necessity of the coordination of the monomer (ethylene) to stabilize the zirconium active specie formed by the reaction of $ZrCl_2$ (ethylpyrone)$_2$ and MAO.

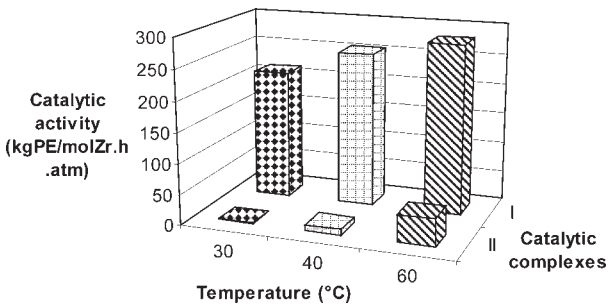

Figure 15. Comparison of the catalytic activities of complexes $ZrCl_2$(ethylpyrone)$_2$ **(I)** and [$ZrCl_2$(methylpyrone)$_2$] **(II)** in the following reaction conditions: [Zr] = 1 μmol, Al/Zr = 2500.

We thank FAPERGS and CNPq for financial support.

REFERENCES AND NOTES

1. Gibson, V. C.; Spitzmesser, S. K. Chem Rev 2003, 103, 283–315.
2. Flisak, Z.; Szczegot, K. J Mol Cat A: Chem 2003, 206, 429–434.
3. Linden, A.; Schaverien, C. J.; Meijboom, N.; Ganter, C.; Orpen, A. G. J Am Chem Soc 1995, 117, 3008–3021.
4. Gueta-Neyroud, T.; Tumanskii, B.; Kapon, M.; Eisen, M. S. Macromolecules 2007, 40, 5261–5270.
5. Gornshtein, F.; Kapon, M.; Botoshansky, M.; Eisen, M. S. Organometallics 2007, 26, 497–507.
6. Fryzuk, M. D.; Jonker, M. J.; Rettig, S. J. Chem Commun 1997, 377–378.
7. Sobota, P.; Przybylak, K.; Utko, J.; Jerzykiewicz, L. B.; Pombeiro, A. J. L.; Silva, M. F. G.; Szczegot, K. Chem Eur J 2001, 7, 951–958.
8. Carone, C.; Lima, V.; Albuquerque, F.; Nunes, P.; Lemos, C.; Santos, J. H. Z.; Galland, G. B.; Stedile, F. C.; Einloft, S.; Basso, N. R. S. J Mol Cat A: Chem 2004, 208, 285–290.
9. Greco, P. P.; Brambilla, R.; Einloft, S.; Stledile, F. C.; Galland, G. B.; Santos, J. H. Z.; Basso, N. S. J Mol Cat A: Chem 2005, 240, 61–66.
10. Frisch, M. J.; Trucks, G. W.; Schlegel, H. B.; Scuseria, G. E.; Robb, M. A.; Cheeseman, J. R.; Zakrzewski, V. G.; Montgomery, J. A., Jr.; Stratmann, R. E.; Burant, J. C.; Dapprich, S.; Millam, J. M.;

Daniels, A. D.; Kudin, K. N.; Strain, M. C.; Farkas, O.; Tomasi, J.; Barone, V.; Cossi, M.; Cammi, R.; Mennucci, B.; Pomelli, C.; Adamo, C.; Clifford, S.; Ochterski, J.; Petersson, G. A.; Ayala, P. Y.; Cui, Q.; Morokuma, K.; Malick, D. K.; Rabuck, A. D.; Raghavachari, K.; Foresman, J. B.; Cioslowski, J.; Ortiz, J. V.; Stefanov, B. B.; Liu, G.; Liashenko, A.; Piskorz, P.; Komaromi, I.; Gomperts, R.; Martin, R. L.; Fox, D. J.; Keith, T.; Al-Laham, M. A.; Peng, C. Y.; Nanayakkara, A.; Gonzalez, C.; Challacombe, C.; Gill, M.; P. M. W.; Johnson, B.; Chen, W.; Wong, M. W.; Andres, J. L.; Gonzalez, C.; Head-Gordon, M.; Replogle, E. S.; Pople, J. A. Gaussian 98, Revision A. 5; Gaussian Inc.: Pittsburgh, PA, 1998.

11. Lee, C.; Yang, W.; Parr, R. G. Phys Rev B 1988, 37, 785–789.
12. Becke, A. D. Phys Rev A 1988, 38, 3098–3100.
13. Dunning, T. H., Jr.; Hay, P. J. In Modern Theoretical Chemistry 3; Schaefer, H. F., III, Ed.; Plenum: New York, 1976; p 1.
14. Hay, P. J.; Wadt, W. R. J Chem Phys 1985, 82, 270–283.
15. Wadt, W. R.; Hay, P. J. J Chem Phys 1985, 82, 284–298.
16. Hay, P. J.; Wadt, W. R. J Chem Phys 1985, 82, 299–310.
17. Wang, X.; Chen, L.; Endou, A.; Kubo, M.; Miyamoto, A. J Organometallic Chem 2003, 678, 156–165.
18. Solomon, E. I.; Lever, A. B. P. Inorganic Electronic Structure and Spectroscopy, Vol. I: Methodology; Wiley: New York, 1999; Solomon, E. I.; Lever, A.B.P. Inorganic Electronic Structure and Spectroscopy, Vol. II: Applications and Case Studies; Wiley: New York, 1999.
19. Loukova, G. V.; Smirnov, V. A. Chem Phys Lett 2000, 329, 437–442.
20. Basso, N. R. de S.; Greco, P. P.; Carone, C. L. P.; Livotto, P. R.; Simplício, L. M. T.; Rocha, Z. N.; da R.; Galland, G. B.; Santos, J. H. Z. J Mol Cat A: Chem 2007, 267, 129–136.
21. Matsui, S.; Fujita, T. Catalysis Today 2001, 66, 63–73.
22. Covoet, D.; Cramail, H.; Deffieux, A. Macromol Chem Phys 1999, 200, 1208–1214.
23. Echevskaya, L. G.; Matsko, M. A.; Mikenas, T. B.; Nikitin, V. E.; Zakharov, V. A. J Appl Polym Sci 2006, 102, 5436–5442.
24. Vyboishchikor, S. F.; Musaev, D. G.; Froese, R. D. J.; Morokuma, K. Organometallics 2001, 20, 309–323.